Measurements of sideward flow around the balance energy

D. Cussol,[1] T. Lefort,[1] J. Péter,[1] G. Auger,[2] Ch. O. Bacri,[3] F. Bocage,[1] B. Borderie,[3] R. Bougault,[1] R. Brou,[1] Ph. Buchet,[4] J. L. Charvet,[4] A. Chbihi,[2] J. Colin,[1] R. Dayras,[4] A. Demeyer,[5] D. Doré,[4] D. Durand,[1] P. Eudes,[6] E. de Filippo,[4,*] J. D. Frankland,[3] E. Galichet,[5,9] E. Genouin-Duhamel,[1] E. Gerlic,[5] M. Germain,[6] D. Gourio,[6,†] D. Guinet,[5] P. Lautesse,[5] J. L. Laville,[2] J. F. Lecolley,[1] A. Le Fèvre,[2] R. Legrain,[4,‡] N. Le Neindre,[1] O. Lopez,[1] M. Louvel,[1] A. M. Maskay,[5] L. Nalpas,[4] A. D. N'Guyen,[1] M. Parlog,[7] E. Plagnol,[3] G. Politi, A. Rahmani,[6] T. Reposeur,[6] M. F. Rivet,[3] E. Rosato,[8] F. Saint-Laurent,[2,§] S. Salou,[2] J. C. Steckmeyer,[1] M. Stern,[5] G. Tabacaru,[7] B. Tamain,[1] L. Tassan-Got,[3] O. Tirel,[2] E. Vient,[1] C. Volant,[4] and J. P. Wieleczko[2]

(INDRA Collaboration)

[1]*LPC Caen (IN2P3-CNRS/ISMRA et Université), F-14050 Caen Cedex, France*
[2]*GANIL (DSM-CEA/IN2P3-CNRS), B.P. 5027, F-14076 Caen Cedex 5, France*
[3]*IPN Orsay (IN2P3-CNRS), F-91406 Orsay Cedex, France*
[4]*DAPNIA-SPhN, CEA/Saclay, F-91191 Gif-sur-Yvette Cedex, France*
[5]*IPN Lyon (IN2P3-CNRS/Université), F-69622 Villeurbanne Cedex, France*
[6]*SUBATECH (IN2P3-CNRS/Université), F-44070 Nantes Cedex, France*
[7]*Nuclear Institute for Physics and Nuclear Engineering, Bucharest, Romania*
[8]*Dipartimento di Scienze Fisiche, Univ. di Napoli, 180126 Napoli, Italy*
[9]*Centre National des Arts et Métiers, F-75141 Paris Cedex 03, France*

(Received 13 July 2001; published 18 March 2002)

Sideward flow values have been determined with the INDRA multidetector for Ar+Ni, Ni+Ni, and Xe+Sn systems studied at GANIL in the 30*A* to 100*A* MeV incident energy range. The balance energies found for Ar+Ni and Ni+Ni systems are in agreement with previous experimental results and theoretical calculations. Negative sideward flow values have been measured. The possible origins of such negative values are discussed. They could result from a more important contribution of evaporated particles with respect to the contribution of promptly emitted particles at midrapidity. But effects induced by the methods used to reconstruct the reaction plane cannot be totally excluded. Complete tests of these methods are presented and the origins of the ''autocorrelation'' effect have been traced back. For heavy fragments, the observed negative flow values seem to be mainly due to the reaction plane reconstruction methods. For light charged particles, these negative values could result from the dynamics of the collisions and from the reaction plane reconstruction methods as well. These effects have to be taken into account when comparisons with theoretical calculations are done.

DOI: 10.1103/PhysRevC.65.044604 PACS number(s): 25.70.−z, 24.10.−i, 25.75.Ld

I. INTRODUCTION

Studies of sideward flow, also called in-plane flow, have been found to provide information on the in-medium nucleon-nucleon interaction. By comparing the experimental results to dynamical calculations, it is possible to constrain the value of the in-medium nucleon-nucleon cross section σ_{nn}, and the incompressibility modulus of infinite nuclear matter K_∞ [1–7]. The so-called balance energy E_{bal} (incident beam energy for which the sideward flow vanishes) has been found to be strongly dependent on σ_{nn} for light systems, and more dependent on K_∞ for heavier systems [7]. For a fixed impact parameter and for a fixed incident energy, the flow parameter value strongly depends on K_∞ [2,8,9]. A dependence on the total isospin of the system has been also observed: keeping the total mass constant, higher values of E_{bal} are extracted for the more neutron-rich systems [10].

A simple interpretation of the sideward flow is that it results from the initial nucleon-nucleon scatterings between projectile nucleons and target nucleons. Within this interpretation, the resulting emissions are centered around the velocity of the nucleon-nucleon center-of-mass frame. The sideward flow is characterized by the flow parameter. It is linked to the mean emission angle in the reaction plane of these direct emissions with respect to the beam axis. At incident energies below E_{bal}, these collisions are sensitive to the attractive part of the nucleon-nucleon interaction: the particles are deflected toward an opposite direction relative to that of the impact parameter vector (the vector perpendicular to the beam axis, pointing from the center of mass of the target to the beam axis, prior to any interaction). In this case, the ''positive'' direction being defined as the direction of the impact parameter vector, the flow parameter is negative. At energies higher than E_{bal}, the initial nucleon-nucleon scatterings are sensitive to the repulsive part of the nucleon-nucleon interaction: the particles are deflected toward the same direction relative to that of the impact parameter vector. In that case the flow parameter is positive. At E_{bal}, the repulsive

*Present address: INFN Corso Italia 57, I-95129 Catania, Italy.
†Present address: GSI, Postfach 110552, D-64220 Darmstadt, Germany.
‡Deceased.
§Present address: CEA, DRFC/STEP, CE Cadarache, F-13108 Saint-Paul-lez-Durance, France.

and the attractive part of the interaction counterbalance: the flow parameter is equal to zero.

But this scheme is indeed too simple. Dynamical calculations [11] have shown that the sideward flow may result from particles emitted at different stages of the reaction. Schematically, one contribution comes from the decay of the so called quasiprojectile and quasitarget, and the other one, from the emission of particles in the first moments of the collision. The relative rate between these two contributions is strongly dependent on the nature of the particle. This may explain the different values of flow actually observed for different types of particles [3,12,13]. In this more realistic frame, the study of the detailed evolution of the sideward flow with the incident energy could shed light on the production mechanism of particles around the nucleon-nucleon velocity.

The measurement of small sideward flow parameter values (typically below 20 MeV/c/nucleon) needs high accuracy and a complete information on each event, which can be achieved by using powerful 4π multi-detectors. Experimentally only positive values of the flow parameter can be measured, since the initial direction of the projectile is unknown, and since the positive direction is defined as the mean direction of particles emitted above the nucleon-nucleon frame velocity. A full understanding of the experimental methods is also needed, in order to correct possible spurious effects.

The aim of this paper is to present the results of the sideward flow analyses on Ar+Ni, Ni+Ni, and Xe+Sn systems from 25A to 95A MeV, and to perform an extensive test of the standard methods used to measure the sideward flow. Sideward flow measurements for the Ni+Ni system at high energies can be found in Ref. [14]. In the first section, the experimental setup will be briefly described. The experimental results will be presented in the second section. The third section will be devoted to the test of various methods used to reconstruct the reaction plane. Conclusions will be drawn in the last section.

II. EXPERIMENTAL SETUP

The experiments were performed at the GANIL facility with the INDRA detector. Target thicknesses were 193 μg/cm^2 of ^{58}Ni for the ^{40}Ar+^{58}Ni experiment, 179 μg/cm^2 of ^{58}Ni for the ^{58}Ni+^{58}Ni experiment, and 330 μg/cm^2 of ^{nat}Sn for the ^{129}Xe+^{nat}Sn experiment. Typical beam intensities were $(3-4)\times10^7$ pps. A minimal bias trigger was used: events were registered when at least three charged particle detectors were fired.

The INDRA detector can be schematically described as a set of 17 detection rings centered on the beam axis. In each ring the detection of charged products was provided with two or three detection layers. The most forward ring, $2°\leqslant\theta_{lab}\leqslant3°$, is made of phoswich detectors (plastic scintillators NE102+NE115). Between 3° and 45° eight rings are constituted by three detector layers: ionization chambers, silicon, and ICs(Tl). Beyond 45°, the eight remaining rings are made of double layers: ionization chambers and ICs(Tl). For the Ar+Ni experiment the ionization chambers beyond 90° were not yet installed. The total number of detection cells is 336 and the overall geometrical efficiency of the INDRA detector corresponds to 90% of 4π. A complete technical description of the INDRA detector and of its electronics is given in Refs. [15,16]. Isotopic separation was achieved up to $Z=3-4$ in the last layer [ICs(Tl)] over the whole angular range ($3°\leqslant\theta_{lab}\leqslant176°$). Charge identification was carried out up to $Z=55$ in the forward region ($3°\leqslant\theta_{lab}\leqslant45°$) and up to $Z=20$ in the backward region ($\theta_{lab}\geqslant45°$). The energy resolution is about 5% for ICs(Tl) and ionization chambers and better than 2% for silicon detectors. The INDRA detector capabilities allow one to carry out an event by event analysis and to determine reliable global variables related to the impact parameter.

III. EXPERIMENTAL RESULTS

A. Event sorting

The first step was to sort events as a function of the violence of the collision. In this paper, we will use the total transverse energy:

$$E_{trans,tot}=\sum_{i=1}^{M} E^i_{k,lab}[\sin(\theta_i)]^2, \quad (1)$$

where M is the charged particle multiplicity of the event and $E^i_{k,lab}$ and θ_i are, respectively, the kinetic energy and the polar angle (with respect to the beam)of the particle i in the laboratory frame. QMD calculations have shown that $E_{trans,tot}$ is a good indicator of the true impact parameter at intermediate energies [17].

In order to sort events, we assumed a geometrical correspondence between $E_{trans,tot}$ and the impact parameter. The cross section of each bin was expressed as an experimentally estimated impact parameter, b_{exp} [18]. The first bin in $E_{trans,tot}$, i.e, the 31.4 mb of the highest values of $E_{trans,tot}$, is linked to b_{exp} between 0 and 1 fm, the second, to b_{exp} between 1 and 2 fm, etc. The last bin corresponds to b_{exp} larger than 8 fm. This procedure has been applied to all detected events. Due to trigger conditions that remove the most peripheral reactions, the estimate of the impact parameter is not very accurate for the lowest values of $E_{trans,tot}$. From now, b_{exp} will refer to the experimentally estimated impact parameter using the total transverse energy. Previous studies [6] have shown that the flow parameter values are weakly sensitive to the exact choice of the sorting variable.

B. Selection of "well measured" events

The next step in the analysis was to select events in which sufficient information was recorded. This was achieved by requiring that the total measured $\Sigma_{i=1}^{M} Z_i V^i_{par}$ (product of the charge Z_i of particle i by its parallel velocity V^i_{par}) be larger than 70% of the initial $Z_{proj}\times V_{proj}$ of the projectile [18].

Since we want to study the dependence on impact parameter of in-plane flow, we checked that this selection conserves the whole impact parameter range. For all systems, we noted that the total transverse energy distribution of selected events covers the whole range of total transverse energy of registered events. If one assumes that the total transverse energy is a good measurement of the violence of the colli-

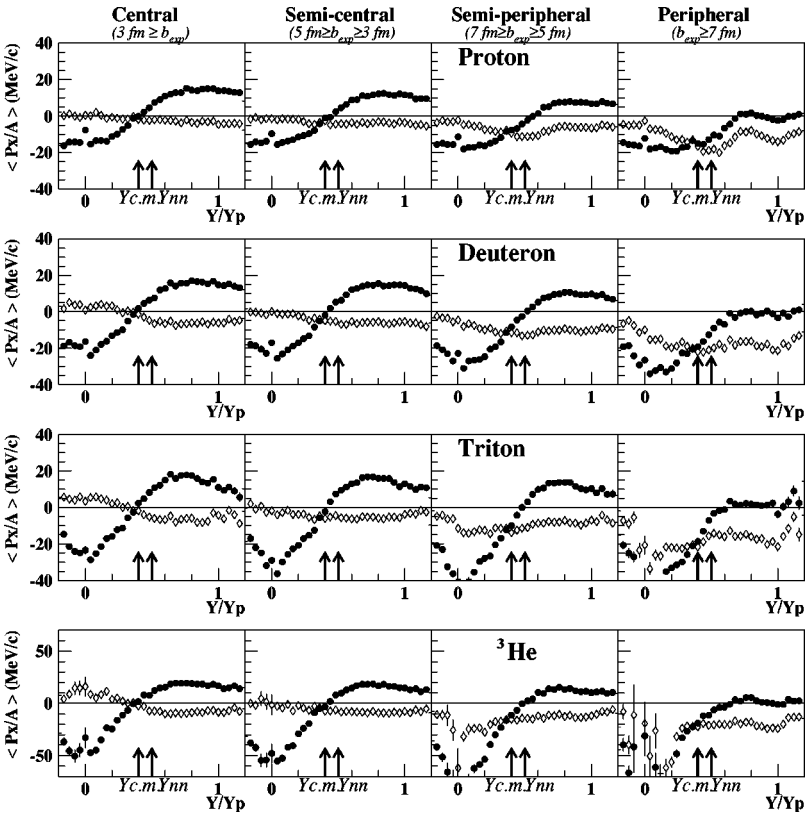

FIG. 1. Variations of P_x as a function of the reduced rapidity Y_r for the Ar + Ni collisions at 74*A* MeV. The first row corresponds to protons, the second to deuterons, the third to tritons, and the fourth to ^{3}He. Each column corresponds to an experimental impact parameter bin, ranging from central (left column) to peripheral collisions (right column). The open circles correspond to the one plane per particle prescription, the full circles, to the one plane per event prescription.

sion, then this result indicates that the whole impact parameter range of registered events is kept in selected events. Indeed, the major part of eliminated events corresponds to some peripheral collisions in which the targetlike fragment (TLF) was not detected, the projectilelike fragment (PLF) was lost in the forward $0°-2°$ beam hole and only few light particles were detected. In this case, $E_{\mathrm{trans,tot}}$ is still correctly measured and since the TLF and PLF transverse energies are very small.

C. Flow parameters

1. Definition

To evaluate the flow parameters, one needs first to determine the reaction plane on a event by event basis. This is done by determining a transverse axis that defines with the beam axis the reaction plane. The transverse momentum method [19] and the momentum tensor method [20] have been used. These methods have been found to be equivalent. As already mentioned in [6], they give a better accuracy on the reaction plane determination than the azimuthal correlations method described in Ref. [21]. With such methods, the transverse axis is by definition oriented on the mean transverse direction of the forward emitted products ($V^i_{\mathrm{par}} > V_{\mathrm{c.m.}}$). Within the standard interpretation of flow, the measured parameters values should be positive. More details about these methods will be given in Sec. V A.

In order to avoid the so called ''autocorrelation'' effect, the particle of interest is usually removed from the reaction plane determination, and a corrective momentum is added to the momentum of other particles [19,22,23]. In this case, one plane per particle is determined. The tests of the methods and the issue of autocorrelations will be presented in Sec. V.

Once the reaction plane is determined, the projection of transverse momenta on the reaction plane can be evaluated. For each reduced rapidity bin $Y_r = Y/Y_{\mathrm{proj}}$, its mean value $\langle P_x/A \rangle$ is calculated, where

$$Y = \frac{1}{2}\ln\left(\frac{1+v_z/c}{1-v_z/c}\right)$$

is the rapidity, v_z the velocity component parallel to the beam in the laboratory frame, and c the light velocity. The flow parameter F is by definition the increase of $\langle P_x/A \rangle$ from $Y = Y_{nn}$ ($Y_r = 0.5$) to $Y = Y_{\mathrm{proj}}$ ($Y_r = 1$) by using the slope of the function $\langle P_x/A \rangle = f(Y_r)$ at midrapidity [23,24]. It reads

$$F = \frac{1}{2}\left(\frac{\partial \langle P_x/A \rangle}{\partial Y_r}\right)_{(Y_r = 0.5)}. \qquad (2)$$

This definition is well established for symmetric systems for which the nucleon-nucleon frame and the center of mass frame coincide. It may not be well suited for very asymmetric systems, especially if the multiplicity of center of mass emissions is higher than the multiplicity of nucleon-nucleon emissions. Nevertheless, we will use the standard definition of the flow parameter in this paper in order to be consistent with previous analyses.

Typical evolutions of $\langle P_x/A \rangle$ with Y_r are shown in Figs. 1 and 2 for Ar+Ni collisions at 74*A* MeV. The rows correspond to the particle types, the columns to the experimental

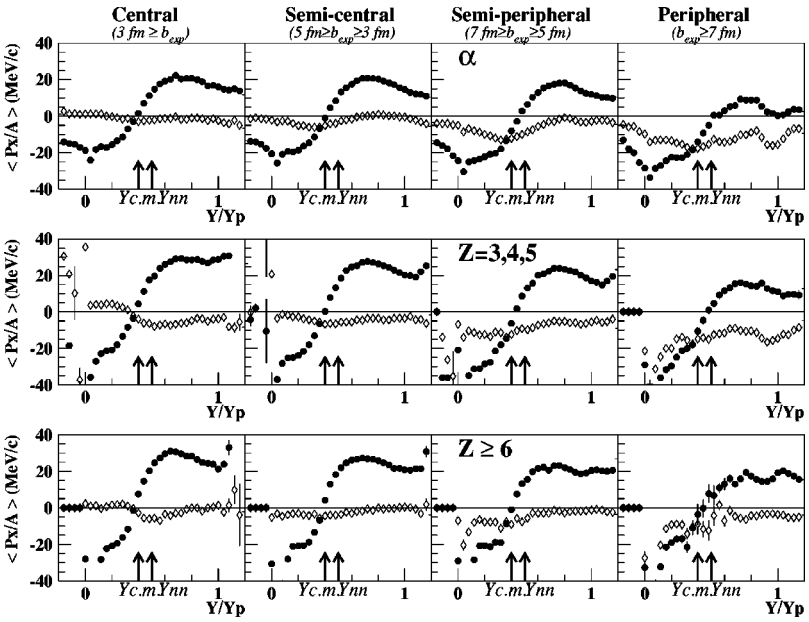

FIG. 2. Same as Fig. 1 for α particles (first row) for $Z=3,4,6$ (second row) and for $Z \geqslant 6$ (third row).

impact parameter bins. The momentum tensor method has been used to reconstruct the reaction plane. For each panel, open circles correspond to one plane per particle (the particle of interest has been removed from the reaction plane reconstruction), full circles to one plane per event (all products are taken into account for the reaction plane determination). For the Ar+Ni system, the balance energy is expected around 80*A* MeV for the central collisions. Therefore, small flow parameter values should be measured at 74*A* MeV.

For the one plane per event prescription (full circles), the slopes at midrapidity are very high and much larger than the expected values. These overestimations are due to the so-called ''autocorrelation effect.'' The flow values determined with the one plane per particle prescription (open circles) are lower and, as a result, in a better agreement with the expected values. Some of them are even negative. Possible explanations of these negative slopes will be given in the following sections.

2. Evolution of the flow parameters with the incident energy.

For the most central collisions ($b_{\mathrm{exp}} \leqslant 3$ fm), the results are shown in Fig. 3 for the Ar+Ni system, in Fig. 4 for the

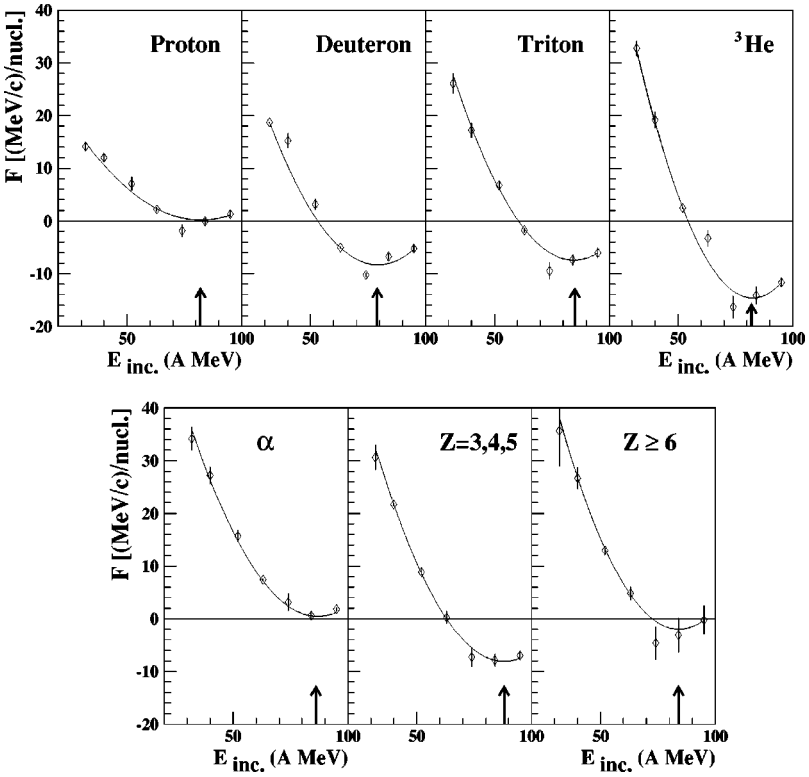

FIG. 3. Variations of the flow parameter F with the incident energy for the most central Ar+Ni collisions ($b_{\mathrm{exp}} \leqslant 3$ fm) and for different particle natures. On each spectrum, the line is a quadratic fit to the experimental value. The balance energy E_{bal} corresponding to the minimum F value is indicated by an arrow. The momentum tensor method with the one plane per particle prescription has been used to reconstruct the reaction plane.

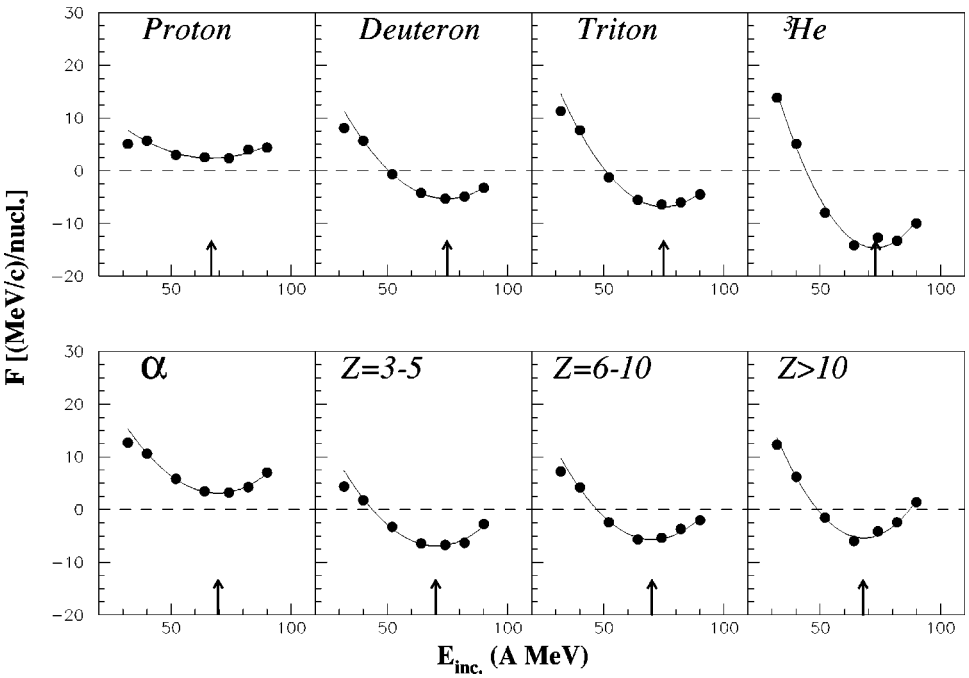

FIG. 4. Variations of the flow parameter F with the incident energy for the most central Ni+Ni collisions ($b_{\mathrm{exp}} \leqslant 3$ fm) and for different particle natures. On each spectrum, the line is a quadratic fit to the experimental value. The balance energy E_{bal}, corresponding to the minimum F value, is indicated by an arrow. The momentum tensor method with the one plane per particle prescription has been used to reconstruct the reaction plane.

Ni+Ni system, and in Fig. 5 for the Xe+Sn system. In the first two experiments, the reaction plane was determined by using the momentum tensor method with the one plane per particle prescription. The flow parameter values has been determined by a linear fit in the Y_r range from 0.4 to 0.6. The errors on flow parameter values have been estimated by changing the Y_r range from 0.35 to 0.65 and from 0.45 to 0.55. The error bars do not appear on the figures when they are smaller that the symbol size.

The evolution of the flow parameter with the incident energy has a typical U shape for all particles. The incident energy that corresponds to the minimum flow value is located around $82 \pm 2)A$ MeV for the Ar+Ni system and around $75 \pm 2A$ MeV for the Ni+Ni system. For both systems, these balance energies do not depend on the particle nature as for systems in Ref. [10]. They are in agreement with theoretical work [2]. These calculation were performed with $K_{\infty} \approx 220$ MeV and $\sigma_{nn} = 0.8\ \sigma_{nn}^{\mathrm{free}}$, where $\sigma_{nn}^{\mathrm{free}}$ is the free nucleon-nucleon cross section.

For the Xe+Sn system (Fig. 5), the results are shown for two reaction plane reconstruction procedures: the momentum tensor method (open diamonds) and the transverse momentum method (stars) with the one plane per particle prescription. As expected, both methods give close results. The U shape is barely seen for ^{3}He and heavy particles ($Z \geqslant 3$). For all particle types, the minimum flow energy is difficult to determine, since the flow parameter weakly depends on the incident energy. Unfortunately, the expected E_{bal} value is around $50A$ MeV, which is the maximum incident energy available for this system. No accurate determination of E_{bal} can be done for this system. The full circles correspond to the momentum tensor method when one plane per event is determined. The flow parameter values are higher than the value obtained with one plane per particle due to the autocorrelation effect. The same behavior is observed with the lighter systems Ar+Ni and Ni+Ni when one plane per event is reconstructed.

But the most striking feature of Figs. 3, 4, and 5 for the one plane per particle prescription is the observation of negative flow parameter values for d, t, ^{3}He and fragments with a charge greater than 3. By definition only positive values are expected. Negative flow parameter values have already been

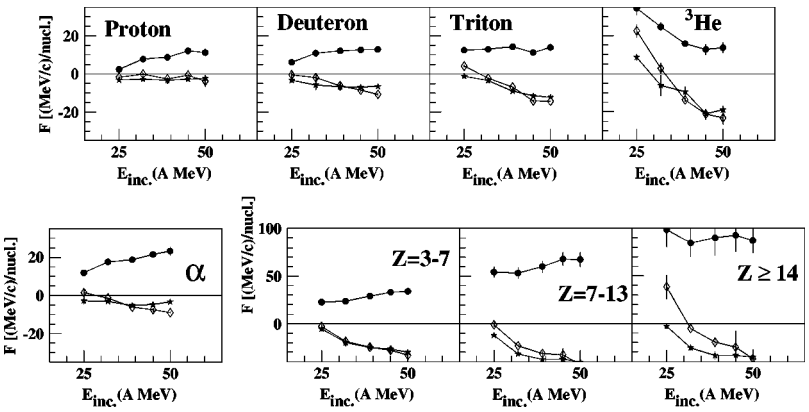

FIG. 5. Variations of the flow parameter F with the incident energy for the most central Xe+Sn collisions ($b_{\mathrm{exp}} \leqslant 3$ fm) and for different particle natures. On each panel, the results of two reaction plane determination are shown: the momentum tensor method (open diamonds) and the transverse momentum method (stars). For both cases, one plane per particle is determined. The full circles correspond to the momentum tensor method when one plane per event is determined.

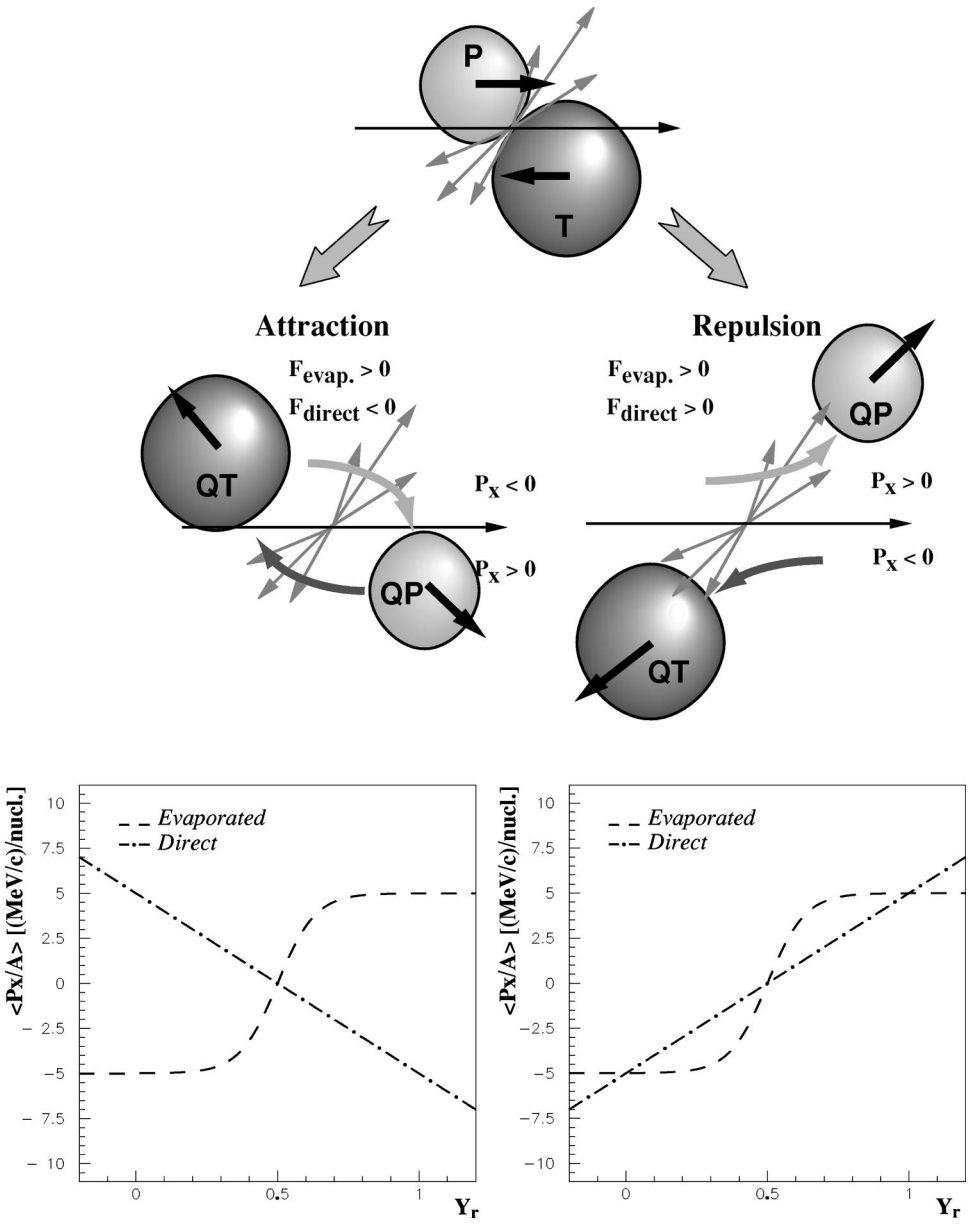

FIG. 6. Schematic explanation of the two possible contributions to the flow parameter. The uppermost picture corresponds to the beginning of the reaction when the projectile P and the target T are touching each other. Arrows correspond to the velocity of ''direct'' (promptly emitted) particles. Middle pictures correspond to the time at which the QP and QT are leaving each other. The lowermost pictures correspond to the expected variation of $\langle P_x/A \rangle$ with Y_r for ''evaporated'' particles (dashed line) and ''direct'' particles (dashed and dotted line) in case of attraction (left column) and bounce-off (right column).

observed in previous studies [25], but no clear explanation was given for this effect. We will propose in the next two sections two possible scenarios for these negative flow values.

IV. THE PHYSICAL EFFECT FOR NEGATIVE FLOW VALUES

A possible explanation for the negative flow values is given by AMD calculations [11]: for light charged particles, the flow of promptly emitted (named ''direct'') particles can be opposite to the flow of ''evaporated'' particles [emitted from the quasiprojectile (QP) and the quasitarget (QT)]. By definition, the reaction plane is oriented positively in the mean direction of forward emitted products. Therefore, negative flow values can be measured.

The direction of the ''direct'' flow in the reaction plane results mainly from screening effects. As shown in Fig. 6, in the first moments of the reaction, ''direct'' nucleons coming from the projectile (target), are screened by the target (projectile) nucleus. For a fixed impact parameter, the orientation of the ''direct'' flow is determined by the geometrical configuration at the touching point and is weakly dependent on the incident energy. It is always aligned in the same direction as the initial orientation of the projectile in the reaction plane. At variance, the direction of the ''evaporated'' flow is aligned on the final directions of the QP. This direction depends strongly on the incident energy, as it will been explained in the next paragraph. Experimental studies have shown that heavy fragments could be emitted by nonevaporative processes, like a neck breakup [26–37]. Since the direction of emission of these fragments is mainly aligned on the QP-QT axis, their flow direction is identical to the so-called ''evaporated'' flow. The contribution of heavy fragments to the flow parameter will be always attributed to the ''evaporated'' component. If one assumes that the observed

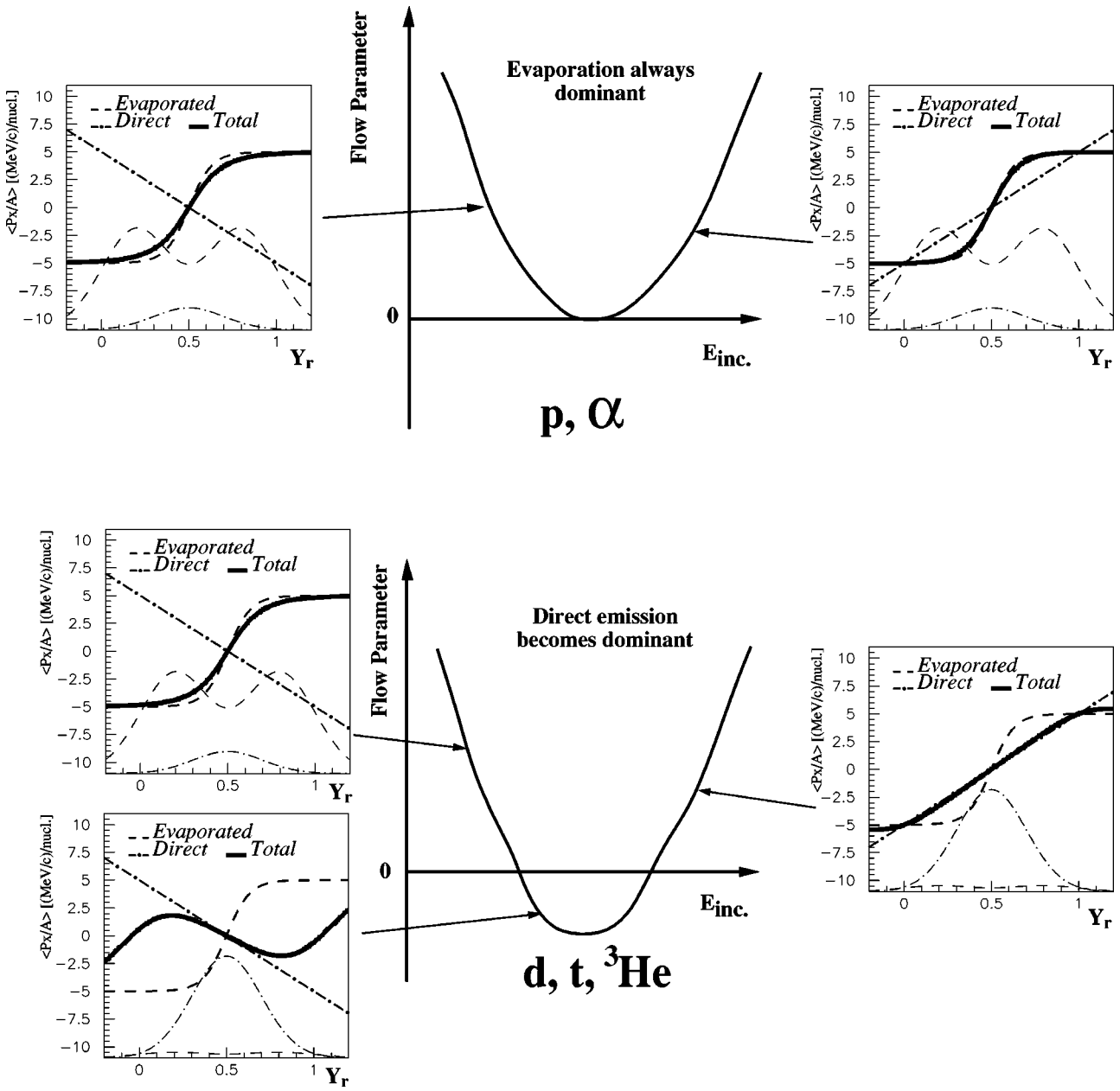

FIG. 7. Expected variations of flow parameter F with incident energy. In the upper panel, the contribution of evaporated particles is always dominant. In the lower panel, the contribution of ''direct'' particles becomes dominant with increasing energy.

flow parameter results only from these two contributions, the evaporated and prompt emissions, a fairly simple picture can be proposed as shown in Fig. 6. The simple pictures shown here are for pedagogical purposes. They do not pretend to reproduce the true process. They are shown to give a feeling of what kind of physical effect could lead to the observation of negative flow parameter values.

At low incident energy, where the attractive part of the nucleon-nucleon interaction dominates, the QP and the QT are deflected to the opposite side relative to their initial directions (left column of Fig. 6). In this case, since $\langle P_x/A \rangle$ is defined to be positive for particles that are deflected on the same side as the QP, the variation of $\langle P_x/A \rangle$ with Y_r is different for the two emissions: a S shape for the evaporated particles with a positive slope around midrapidity (dashed line in the lower left picture of Fig. 6) and a straight line with a negative slope for the direct particles (dashed and dotted lines).

At higher energies, where the repulsive part on the interaction is dominant, the QP ''bounces'' on the QT (right column of Fig. 6). In this case, the variations of $\langle P_x/A \rangle$ with Y_r give a positive slope around midrapidity for the two emissions as shown in the lower right panel of Fig. 6. The observed variation of $\langle P_x/A \rangle$ with Y_r is a combination of these two contributions with their associated Y_r distributions.

Such combinations are schematically shown in Fig. 7. For each side panel, the original $\langle P_x/A \rangle$ evolution of the ''direct'' particles (straight dashed and dotted line) and its corresponding Y_r distribution (dashed and dotted Gaussian distribution) are plotted. The $\langle P_x/A \rangle$ contribution (''S'' shape)

and the Y_r distribution of ''evaporated'' particles (sum of two gaussian distributions) are plotted as dashed lines. The resulting evolution of $\langle P_x/A \rangle$ corresponds to the thick line. It is simply obtained by summing the two $\langle P_x/A \rangle$ contributions weighted by their corresponding Y_r distributions.

If the contribution of evaporated particles is dominant, then the resulting flow parameter value is always positive (upper row of Fig. 7). The S shape is weakly affected by the contribution of direct emissions. At variance, if direct emissions become dominant (lower row of Fig. 7), then a negative flow value can be obtained. At low incident energies, the evolution of $\langle P_x/A \rangle$ with Y_r is dominated by the evaporated particles. When direct emissions become dominant, the evolution of $\langle P_x/A \rangle$ with Y_r follows the one of the direct particles, and the S shape is strongly deformed. Negative slopes can be found at midrapidity, i.e., negative flow parameter values.

This explanation is very tempting for the light charged particles. Deuterons, tritons, and ^{3}He are predominantly emitted in the midrapidity regions, whereas protons and α particles are emitted as much by the QP and QT as by the midrapidity emissions [38,39]. At the same time, positive flow values are measured for α particles and protons and negative values for deuterons, tritons, and ^{3}He (see Figs. 3, 4, and 5). Both experimental features support the above interpretation. But this does not explain the negative values observed for the heavier fragments. Within the simple interpretation of sideward flow, the emission of fragments via cluster-cluster collisions of preexisting fragments in both bulk partners has a very low probability. As already mentioned, for PLF and the TLF, this observation is even in contradiction to the reaction plane orientation, which is always oriented along the direction of the quasiprojectile. The solution of this puzzle has to be found elsewhere.

Previous studies [23] have shown that the reaction plane determination method and the associated issue of autocorrelations could strongly disturb the measurement of flow parameter. Before attributing the observation of negative flow parameter values to physical effects, one has first to be sure that these negative values are not due to the analysis methods. The next section is devoted to the test of reaction plane determination methods. The origins of the so-called autocorrelation effects will also be studied.

V. TEST OF THE REACTION PLANE DETERMINATION METHODS

A. Reaction plane estimation

Let us now briefly describe three commonly used methods: the transverse momentum method [19], the momentum tensor method [20], and the azimuthal correlations method [21]. From now on, the Oz axis is the beam axis, the Ox axis is the axis in the reaction plane, which is perpendicular to the beam axis and Oy axis is the axis perpendicular to the reaction plane. The transverse momentum method, explained in detail in Ref. [19], is based on the fact that the sum of transverse momenta of particles emitted by the quasiprojectile $\vec{P}_{\rm QP}$ is opposite of the sum of the transverse momenta of particles emitted from the quasitarget $\vec{P}_{\rm QT}$. This is valid within the binary mechanism hypothesis, where the midrapidity contribution is negligible. Those vectors belong to the reaction plane. In order to maximize the efficiency of the method, one has to calculate the difference of the two vectors $\vec{Q}=\vec{P}_{\rm QP}-\vec{P}_{\rm QT}$. Usually, $\vec{Q}$ is determined in the following way:

$$\vec{Q}=\sum_{j=1}^{N} \omega_j \vec{P}_j^{\perp}, \tag{3}$$

where N is the total number of particles in the event, $\vec{P}_j^{\perp}$ is the transverse momentum of particle j, and ω_j a weight defined as follows:

$$\omega(Y_r)=\begin{cases} -1 & \text{if} \quad Y_r - Y_{r\text{c.m.}} < -\delta \\ 0 & \text{if} \quad -\delta \leqslant Y_r - Y_{r\text{c.m.}} \leqslant \delta \\ 1 & \text{if} \quad Y_r - Y_{r\text{c.m.}} > \delta \end{cases} \tag{4}$$

or

$$\omega(Y_r)=Y_r - Y_{r\text{c.m.}}, \tag{5}$$

where Y_r is the reduced rapidity of the particle, $Y_{r\text{c.m.}}$ the center of mass reduced rapidity (close to the reduced rapidity of the nucleon-nucleon frame Y_{rnn} for the symmetric systems), and δ a parameter that allows us to remove the midrapidity particles from the estimation of the reaction plane. $\vec{Q}$ defines the reaction plane with the beam direction. With this definition, the reaction plane is systematically oriented along the quasiprojectile direction.

Another way to estimate the reaction plane is to calculate and diagonalize a tensor $T_{\mu,\nu}$. The beam axis defines the reaction plane with the eigenvector corresponding to the highest eigenvalue. As for the transverse momentum the reaction plane is oriented along the direction of the quasiprojectile. The tensor is defined in the following way:

$$T_{\mu\nu}=\sum_{j=1}^{N} \Omega_j P_j^{\mu} P_j^{\nu} \quad \text{with} \quad \mu,\nu=x,y,z, \tag{6}$$

where P_j^{μ} is the momentum component along the μ axis ($\mu=x,y,z$) for the particle j. Ω_j is a weight that is usually set to the inverse of the mass A_j of the particle $\Omega_j=1/A_j$ (energy tensor).

The azimuthal correlation method is based on the following observation: in case of strong in-plane emission (high flow-parameter value), the sum of the distances of particle momenta with respect to that plane are minimum [21]. This sum D^2 is calculated as follows:

$$D^2=\sum_{j=1}^{N}\left[(P_j^x)^2+(P_j^y)^2-\frac{(P_j^x+aP_j^y)^2}{1+a^2}\right], \tag{7}$$

where P_j^x and P_j^y are the transverse momentum components along the Ox and Oy axis, respectively, and $a=\tan(\varphi)$,

where φ is the angle of the reaction plane relative to the Ox axis. Experimentally, one has to find the value of φ that minimizes D^2. With this method, the orientation of the reaction plane is not defined. One has to use the transverse momentum method to find it. In the case of strong out-of-plane particle emission (squeeze-out), the estimated reaction plane angle is wrong by $\pi/2$.

B. Testing procedure

Since the flow parameter is obtained from the average value of the transverse momentum projection on the reaction plane, one has to rebuild this plane from the experimental data. We have checked the reliabilities of the three reaction plane reconstruction methods. The general procedure of the test is the following: a known flow parameter value F is set for a sample of generated events; then the reaction plane estimation method is applied on that sample and the so-called ''experimental flow parameter'' $F_{\rm exp}$ is determined. A method is considered effective if the experimental value $F_{\rm exp}$ is equal or close to the initial one $F_{\rm init}$. This allows us to also check the additional disturbance introduced by the experimental setup compared to the method itself.

To set the flow parameter value F to an event, an in-plane component P_x^a is added to the transverse momentum of each particle, similarly to the procedure used in Ref. [23]. The amplitude of this in-plane component depends on the reduced rapidity of the particle:

$$P_x^a(F,Y_r) = \begin{cases} -\dfrac{AF}{2} & \text{if} \quad Y_r < 0.25 \\ 2AF(Y_r - 0.5) & \text{if} \quad 0.25 \leqslant Y_r \leqslant 0.75 \\ \dfrac{AF}{2} & \text{if} \quad Y_r > 0.75 \end{cases} \tag{8}$$

where F is the flow parameter value to be set, Y_r is the reduced rapidity of the particle, A its mass, and $P_x^a(F,Y_r)$ the in-plane component.

The test has been performed on two systems, Ar+Ni at 74A MeV and Xe+Sn at 50A MeV. These two systems have been studied with INDRA and their comparison allows us to check the effect of the mass of the system on the transverse flow measurement. These energy values have been chosen because they are close to the expected balance energy. For each system, 15 000 events have been generated using the SIMON code, whose entrance channel includes a preequilibrium emission of protons and neutrons [40]. SIMON is not used to reproduce the experimental data, but rather as an event generator. The goal is to check how the reaction plane reconstruction methods react in a well-defined situation. In this test, only the most central collisions have been used. The flow parameters for the different particle types are not exactly zero but close to zero, and differ from a particle type to another. The effect of the addition of the P_x^a component is to add the value of F to the original value of the flow parameter, giving a $F_{\rm init}$ value. This procedure will allow us to study the effects of the different reaction plane reconstruction methods on flow parameter measurements, as in Ref. [23].

C. One plane per event or one plane per particle?

Since the transverse momentum is used both for the reaction plane estimation and for the projection, auto-correlations are expected (see full circles in Figs. 1 and 2). Autocorrelation effects are also amplified by the loss of information due to a nonperfect detection. The usual way to solve this problem is to remove the particle that has to be projected from the estimation of the reaction plane. Thus, an additional corrective component $\vec{P}_j^{\rm cor}$ is added to the momentum of the remaining particles in order to ensure the conservation of the total momentum. Its definition is the following:

$$\vec{P}_j^{\rm cor} = -\frac{A_j}{M} \vec{V}_i \tag{9}$$

$$\sum_{k=1,k\neq i} A_k$$

where i is the removed particle, $\vec{V}_i$ its velocity, A_j the mass of particle j $(j \neq i)$, and M the event multiplicity. In this case, one plane is determined for each particle of the event.

Two prescriptions have been used for the methods described in Sec. V A. In the first one, one plane per event is determined. This allows to check the effect of the autocorre lations with respect to the method used. In the second one, one plane per particle is determined, in order to test the efficiency of the correction.

1. Azimuthal dispersion between the true reaction plane and the reconstructed one

To compare the relative efficiencies of these methods, the distribution of the angular azimuthal difference $\Delta\Phi$ between the true and the reconstructed reaction plane directions has been studied. Such distributions have been already shown (see Fig. 6 of Ref. [6]).

The observed mean value $\langle \Delta\Phi \rangle$ is zero. The accuracy of the reaction plane determination is estimated with the standard deviation $\sigma(\Delta\Phi)$ of these distributions as a function of the added flow parameter value F. Figure 8 shows such evolutions of $\sigma(\Delta\Phi)$ with F. F has been used instead of $F_{\rm init}$ because the $F_{\rm init}$ values are different from one particle type to another, whereas the same F value has been added to all particles. The upper row corresponds to the Ar+Ni system, the lower row to the Xe+Sn system. The left column corresponds to the case when one plane per particle is determined and the right column to the one plane per event prescription. No significant difference is found between these two prescriptions. For all methods and systems, the dispersion $\sigma(\Delta\Phi)$ decreases when F increases. For small F values, the different methods give slightly different results because the initial flow parameter is not zero. As expected, the reaction plane determination is more accurate in the case of strong in-plane emission. For both systems, the transverse momentum method and the tensor method give similar accuracies, whereas for the azimuthal correlation method the dispersion

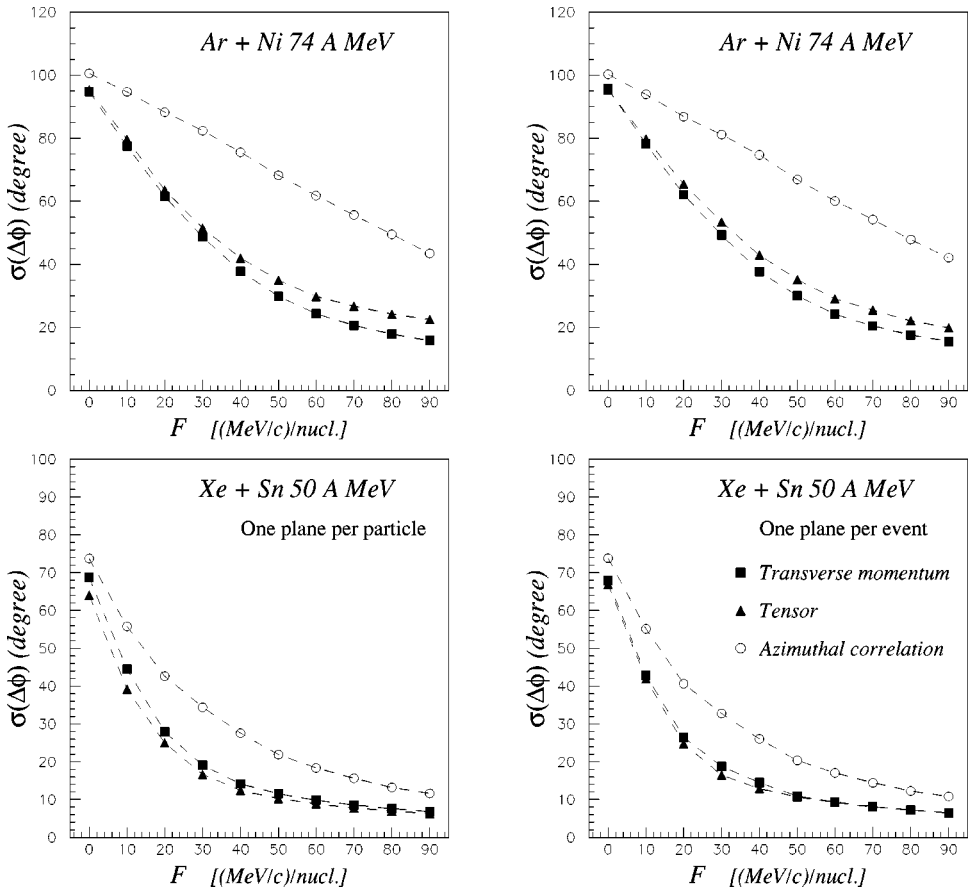

FIG. 8. Accuracy on the reaction plane estimation obtained as a function of the initial flow parameter value F_{init}. This was obtained by using the SIMON code for the Ar+Ni system at 74*A* MeV (upper row) and for the Xe+Sn system at 50*A* MeV (lower row). The left column corresponds to the one plane per particle prescription and the right column to the one plane per event prescription. The squares correspond to the transverse momentum method, the triangles to the momentum tensor method, and the open circles to the azimuthal correlation method.

is systematically higher for all F values. For the Xe+Sn system, the values of $\sigma_{\Delta\Phi}$ are smaller than those for the Ar + Ni system.

From these observations, three main conclusions can be drawn: (i) the azimuthal dispersion of the reconstructed reaction plane is the same for the one plane per particle and one plane per event prescriptions; (ii) similar to the conclusion of Ref. [6], the azimuthal correlation method is less accurate than the two other methods, even at low F_{init} values; (iii) the higher the mass of the system and the higher the F_{init} value, the more accurate the reaction plane reconstruction.

Surprisingly, no difference is seen in $\sigma(\Delta\Phi)$ between the one plane per particle and the one plane per event prescriptions, whereas strong discrepancies are seen for the $\langle P_x/A\rangle = f(Y_r)$ curves (Figs. 1 and 2). One has to keep in mind that in the present case, only the deviation from the true reaction plane is studied. For the $\langle P_x/A\rangle = f(Y_r)$ curves, the combined effects of the reaction plane reconstruction accuracy and of the projection of transverse momenta on the reconstructed reaction plane are present.

2. Measured flow parameter versus initial flow parameter

For the transverse momentum method, the dependence of F_{exp} on the initial value of the flow parameter is shown in Fig. 9 in the case of one plane per particle (left column) and in case of one plane per event (right column). For one plane per particle, the procedure used to remove autocorrelations seems to be efficient for H isotopes. For heavier particles, F_{exp} is systematically below F_{init}. This underestimation increases with increasing charge. For a given F_{init} value, the underestimation is lower for the Xe+Sn system than for Ar +Ni. Finally, the amplitude of this underestimation decreases with increasing value of F_{init}.

With one plane per event (right column of Fig. 9), F_{exp} values are systematically larger than F_{init} values due to the autocorrelation effects mentioned above. For a fixed F_{init} value, the overestimation increases with decreasing charge of the particle. Here again, the amplitude of the overestimation diminishes for higher values of F_{init} and with increasing mass of the system.

For the momentum tensor method, results are shown in Fig. 10 for one plane per particle (left column) and for one plane per event (right column). The same trends are observed as for the transverse momentum method. The autocorrelation effects are smaller in the case of one plane per event.

For the azimuthal correlation method (Fig. 11), the same trends are observed as for the two other methods. The main difference is a somewhat larger underestimation of the flow parameter value.

3. Influence of the experimental setup

Part of the anti- or autocorrelation may be related to the detector efficiency. In order to probe the effect of the experimental setup, the INDRA filter has been applied on the generated events. The INDRA filter is a sophisticated software that simulates the response of the detector. For each particle,

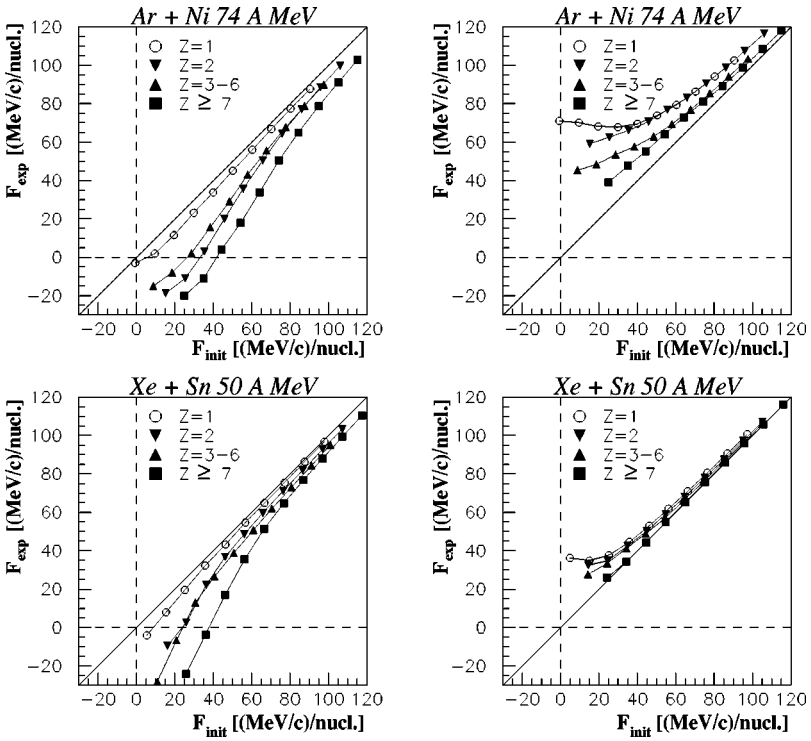

FIG. 9. Correlation of the measured flow parameter value F_{exp} and the initial flow parameter value F_{init} in the framework of the SIMON code. The transverse momentum method has been used and one plane per particle has been calculated. The upper panel corresponds to the Ar+Ni system at 74*A* MeV and the lower panel to the Xe+Sn system at 50*A* MeV. The left column corresponds to the one plane per particle presciption and the right column to the one plane per event presciption.

the energy losses in each layer of the detector are calculated. An identification procedure similar to the experimental one is then applied on the energy losses giving back the charge and the energy of the detected particle. Doing this, multiple hits in a detector are treated in the same way they are treated in the experiment. This procedure allowed the reproduction of the angular and energy thresholds observed experimentally.

The reaction plane is then reconstructed from the so called filtered events. In Fig. 12, the correlation between F_{exp} and F_{init} is plotted for the momentum tensor method with the one plane per event prescription. For the two systems studied here, the results are very similar to those obtained with a perfect detection (see the right column of Fig. 10). The measured flow values are above the initial ones for the Ar+Ni system and close to the initial ones for the Xe+Sn system. The detector has a weaker effect than the reaction plane determination procedure. This conclusion is identical to those made in Ref. [23] for a 4π array that had higher thresholds.

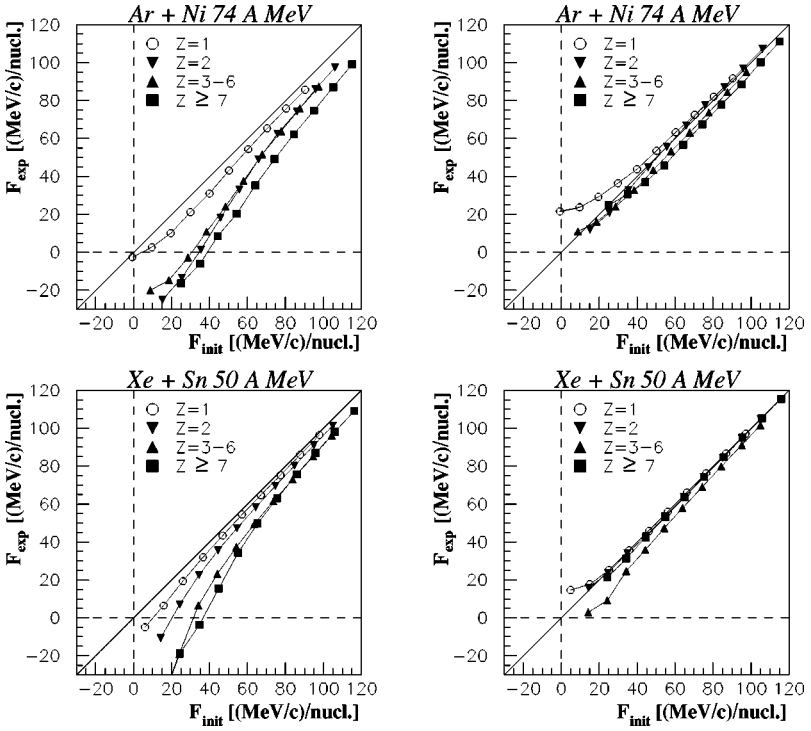

FIG. 10. Same as Fig. 9 by using the momentum tensor method.

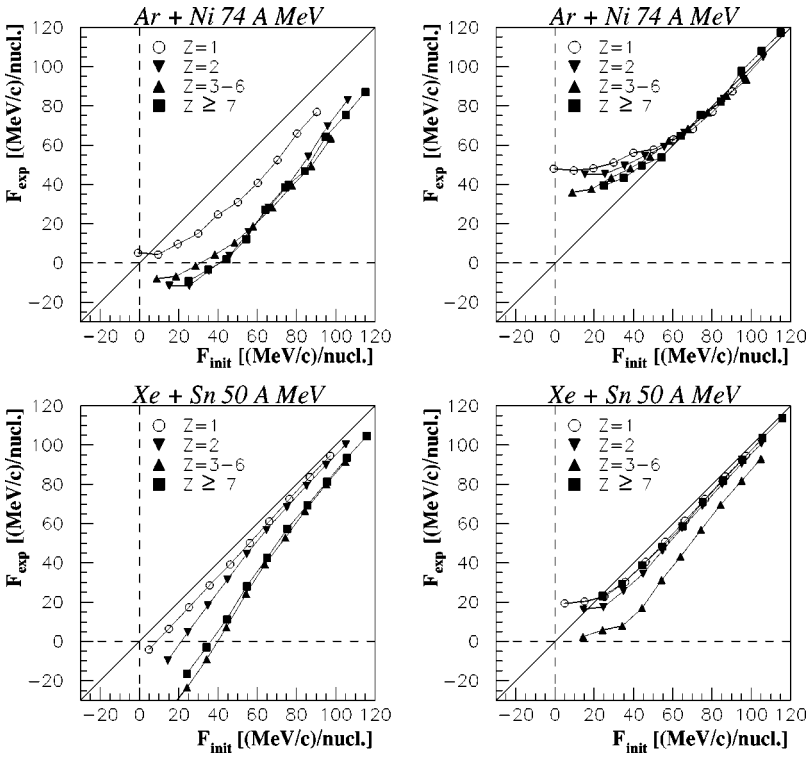

FIG. 11. Same as Fig. 9 by using the azimuthal correlation method.

4. Conclusions of the simulations

The following conclusions can be drawn from the previous study:

(i) removing the particle of interest from the reaction plane introduces an anticorrelation that is not counterbalanced by adding a corrective momentum $\vec{P}_j^{\,\mathrm{cor}}$ to the momentum of other particles. The anticorrelation effect leads to an underestimation of sideward flow values.

(ii) When one plane per particle is determined, the amplitude of the anticorrelation is higher for small F_{init} values, for heavy particles, and for small system size.

(iii) When one plane per event is determined, the amplitude of the autocorrelation is higher for small F_{init} values, for light particles, and for small system size.

(iv) For all methods, for the one plane per event prescription, the autocorrelation effect leads to an overestimation of the flow parameter value. This overestimation is minimum for the momentum tensor method.

(v) The best results are obtained for the momentum tensor method with the one plane per event prescription.

(vi) Detection effects are weaker than effects induced by the procedures used to reconstruct the reaction plane.

One could conclude from these simulations that the best method to measure small sideward flow values is the momentum tensor method with one plane per event. Unfortunately, the simulation is too simple compared to the experimental situation. We remind the reader that in this simulation, the midrapidity contribution is only present for protons and neutrons. This is why the autocorrelation effect is mainly seen for protons in the simulation. In the experimental data, the midrapidity emission is also made of heavier particles [38,39]. The autocorrelation effect is seen for all particles for the Ar+Ni system (full circles in Figs. 1 and 2) as well as for the Xe+Sn system (full circles in Fig. 5). In the latter case, the flow parameter is weakly dependent on the incident energy. Therefore, from the experimental results, it turns out that the autocorrelation effects are strong. In other words, qualitative effects may be understood thanks to the simulations, but quantitative estimations of the corrections required in the data are difficult to realize from these simulations. Such a correction may be done if the autocorrelation effect is well understood. The study of the origins of the autocorrelation effect is done in the next section.

D. Origin of the autocorrelations

These studies show us that the methods developed at high energies, where high values of sideward flow are measured, are not well suited for intermediate energies where the flow parameter values are typically around or below 30 MeV/c/nucleon. The amplitude of the anti- or autocorrelations depends also on the nature of the particle. Let us try nevertheless to identify the origin of the autocorrelations at intermediate energies.

First of all, one has to make some remarks. If a method would be able to reconstruct perfectly the reaction plane from the momentum of all particles, no autocorrelation effect would be seen. This is shown for example in the right column of Fig. 10 for the Xe+Sn system. The experimental flow parameter F_{exp} is very close to F_{init} for F_{init} values above 20 MeV/c/nucleon, although the momenta of all particles have been used to calculate the momentum tensor. This is quite unexpected since for high F_{init} values, the transverse momenta values are large. The autocorrelation effect should be maximum for high F_{init}. The usual explanation of the autocorrelation effect does not seem to be the right one. If so, where does this autocorrelation effect come from? Since the

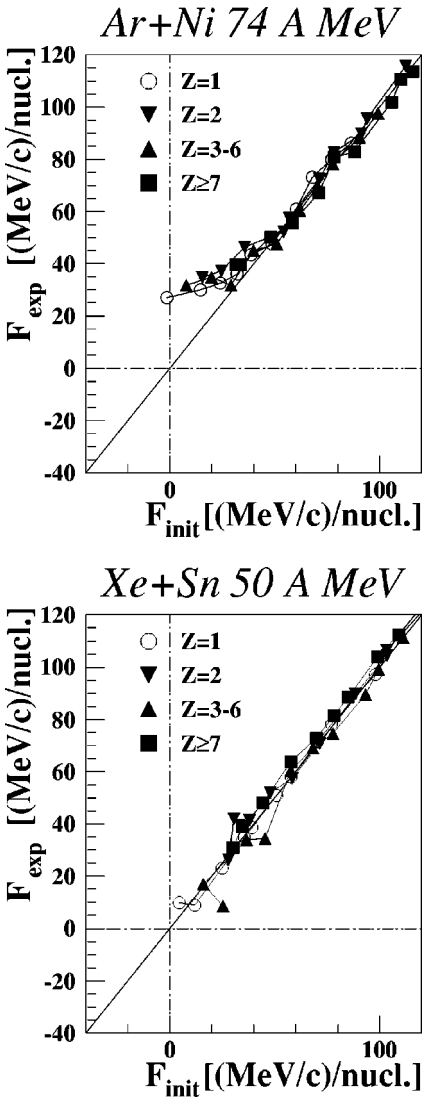

FIG. 12. Same as Fig. 10 right column but the events have been affected by the INDRA filter.

azimuthal correlation method is less accurate than the two other ones, the origin of the autocorrelations will not be checked for this method.

1. Autocorrelations for the transverse momentum method

In the transverse momentum method, one assumes that the particles emitted above $Y_{\mathrm{c.m.}}$ are all coming from the decay of the quasiprojectile (QP), and those emitted below $Y_{\mathrm{c.m.}}$ are all coming from the decay of the quasitarget (QT). But at intermediate energies, the contributions from the QT, the QP, and the midrapidity area are mixed, especially for the most violent collisions [38,39]. In addition, for the most central collisions, the azimuthal angular distributions are rather flat and no privileged direction can be clearly seen. Therefore a wrong weight may be attributed to the particles, and the estimated reaction plane may have nothing to do with the true one. In this case, the reconstructed reaction plane may be oriented along the particles with the highest momenta.

On the other hand, if the right weight was attributed to the right particles, this effect should vanish. This can be checked in the simulation, for which the origin of particles is known. The results are shown in Fig. 13. In this simulation, a pure binary scenario has been assumed: the first stage of the collision leads to the formation of a quasiprojectile and a quasitarget both deflected in the reaction plane, without any preequilibrium emissions. One plane per event is determined, using the transverse momentum method, and the weight of the particles is attributed according to their origin: $+1$ for the particles emitted by the quasiprojectile and -1 for those emitted by the quasitarget. It is seen that the effect of autocorrelation is removed, even for the smaller flow values. The so called autocorrelation effect comes from a loss of information (the origin of the detected particles), instead of the use of the transverse momenta in both the reaction plane determination and in the projection.

In the experiment, the exact knowledge of the origin of the particle is impossible, especially for the most damped reactions. In addition the collisions are not purely binary due to prompt emissions. The promptly emitted particles carry a part of the total tansverse momentum and the QP and QT are hence pushed out of the reaction plane. In the experiment, the perfect determination of the reaction plane using the tranverse momentum method is very difficult, especially for the central collisions.

2. Autocorrelations for the momentum tensor method

For the momentum tensor method, the origin of autocorrelation effects can be understood using a simple test. Let us consider the case where a quasiprojectile of mass number A splits into two equal size fragments and the quasitarget of the same mass number A remains unchanged. The quasiprojectile and the quasitarget are deflected in the reaction plane. The axis joining their center of mass has an angle θ_{deflec} with respect to the beam axis (see Fig. 14). The axis joining the two fragments issued from the splitting of the quasiprojectile has an angle θ_{split} with respect to the beam direction and an angle ϕ_{split} with respect to the reaction plane. The relative velocity between the quasiprojectile and the quasi-target is V_r and the relative velocity between the two fragments of the quasiprojectile is αV_r. A scheme of the described configuration is presented in Fig. 14.

The momentum tensor of such a simple case can be calculated, and one can study the azimuthal angular difference $\Delta\phi$ between the reconstructed reaction plane and the true one. The direction of the reaction plane is defined in the plane transverse to the beam axis, displayed in the right panel of Fig. 14. In this panel, the QT is by definition in the reaction plane but the two splitting fragments are out of the plane.

The first key variable is α. When its value is small (close to zero), the QP-QT axis is obviously the main axis and the reaction plane is perfectly determined. But when the α value is big enough, the axis between the two splitting fragments may become the main axis. In this case, the reconstructed reaction plane direction may be dependent on the splitting direction ϕ_{split}, which is the second key variable.

In Fig. 15, the evolutions of $\Delta\phi$ as a function of α and ϕ_{split} are displayed. The angles $\theta_{\mathrm{deflect}}$ and θ_{split} are set, respectively, to 10° and 40°. Similar pictures are obtained for

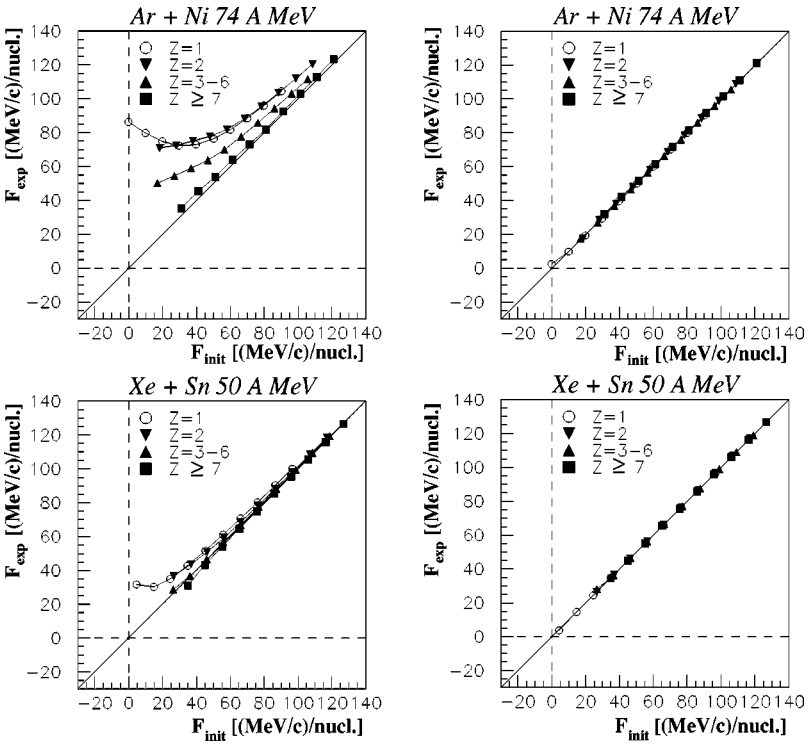

FIG. 13. Correlation of the measured flow parameter value F_{exp} and the initial flow parameter value F_{init} in the framework of the SIMON code assuming a pure binary scenario (excited QP and QT only). Left column: the transverse momentum method has been used and the weights are determined according to the reduced rapidity of the particle. Right column: the weights are set according to the true origin of the particle. One plane per event has been calculated.

other $\theta_{\mathrm{deflect}}$ and θ_{split} values. For large enough values of α $\Delta\phi$ is strongly dependent on ϕ_{split}. For low values of α, i.e. small relative velocities of the two fragments compared to the relative velocities of the quasiprojectile and the quasitarget, $\Delta\phi$ does not depend on ϕ_{split} and is equal to zero. The two out-of-plane fragments do not introduce much pertubations on the reconstruction procedure. The direction of the reconstructed reaction plane is mainly determined by the QT. The reaction plane is therefore well estimated. On the other hand, when α is larger than 1, the reaction plane is mainly determined by the two out-plane fragments. The direction of the reconstructed reaction plane is therefore correlated to the splitting direction. In the experiment, this last configuration is similar to the most violent (central) collisions but with a larger multiplicity.

If the two fragments issued from the splitting of the quasiprojectile were gathered before applying the momentum tensor method, the reaction plane would be perfectly determined whatever the fragmenting configuration. That means that if the origin of the fragments is known, on can determine perfectly the reaction plane by grouping the fragments coming from the same source in a single fragment. The results of the momentum tensor method depend on the way the fragments are gathered. As for the tranverse momentum method, a perfect determination of the reaction plane by using the momentum tensor method is very difficult in the experiment.

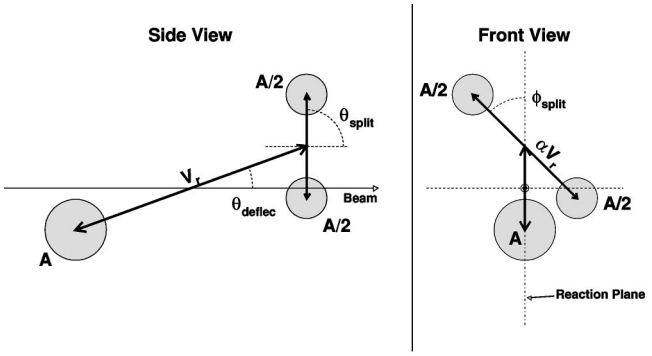

FIG. 14. Scheme of the configuration used to test the autocorrelation effect for the momentum tensor method (see text).

E. Discussion

For incident energies around the balance energy, the standard methods used for the reaction plane reconstruction are not well suited. Whatever the method used, the one plane per event prescription leads to an autocorrelation effect, i.e., a large overestimation of the flow parameter values. At variance, the one plane per particle prescription induces an anticorrelation effect which gives an underestimation of the flow parameter.

This indicates that the negative flow values observed in experimental data can be attributed to the used reconstruction methods, especially for the heaviest fragments. For the light charged particles, the physical effect cannot be completely ruled out, since positive values of flow are observed for α particles, whereas negative values are expected if the reaction plane determination methods effects are dominant. For such particles, the two effects are probably mixed and more detailed studies have to be performed to establish their relative weights in the observed values. To obtain the true flow parameter values, one has to understand the autocorrelation effects in order to correct them accurately.

But understanding the origin of the autocorrelation effects is a complicated task. To correct them, a complete knowledge of the origin of particles is needed. This can be

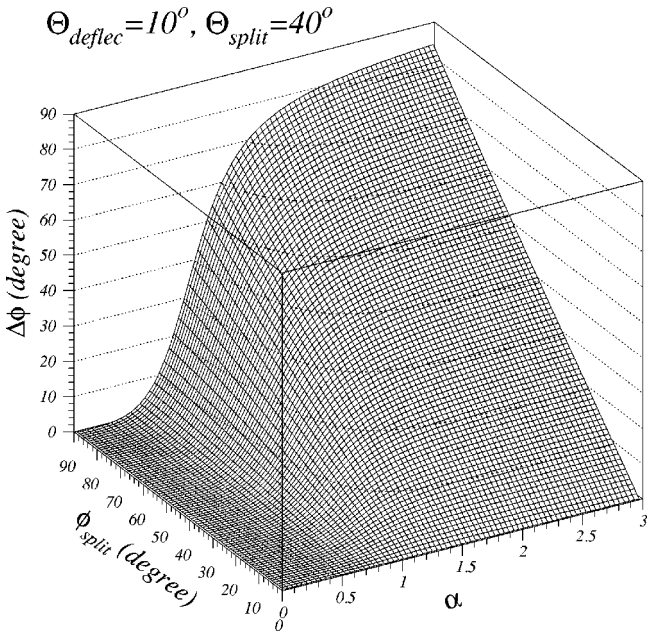

FIG. 15. Variations of the angle ϕ between the true reaction plane and the estimated one by using the momentum tensor method for $\theta_{\text{deflect}}=10°$ and $\theta_{\text{split}}=40°$. See text for details.

achieved only for the less violent collisions and/or at higher energies where the mixing between the different contributions is weak. For the most violent collisions, such knowledge is unreachable unless assumptions are made. But in this case, the flow values obtained may only result from these assumptions.

Since the correction of experimental data seems to be impossible, it could be easier to apply the experimental filter and the analysis procedure on theoretical calculations. Most of the available dynamical calculations have to evolve to enable this procedure, since most of them are following the time evolution of the one body density. More precisely, the dynamical calculations should include the proper description of particle and fragment formation.

VI. CONCLUSIONS

The in-plane flow parameter has been determined for the Ar+Ni collisions from 32*A* MeV to 95*A* MeV, for the Ni+Ni system from 32*A* MeV to 90*A* MeV, and for the Xe+Sn system from 25*A* MeV to 50*A* MeV. For central collisions, the balance energies are equal to $(82 \pm 2)A$ MeV for the Ar+Ni system and $(75 \pm 2)A$ MeV for the Ni+Ni system. For the Xe+Sn system, the balance energy is around 50*A* MeV, but experiments at higher incident energies have to be performed to confirm the result. These values are in agreement with the systematics of balance energies found in other experiments. This systematics has been reproduced by a dynamical model assuming $K_\infty \approx 220$ MeV and $\sigma_{nn} = 0.8\ \sigma_{nn}^{\text{free}}$ [2]. As already observed, the balance energy weakly depends on the particle nature. For these central collisions, negative flow values are observed for both systems. Two different explanations are proposed for these negative values.

The first one, supported by transport model calculations, attributes this effect to the relative importance between the prompt emission and the evaporative one. A negative flow parameter value can be observed if the prompt emission is dominant. This explanation seems to be satisfactory for the light particles. Deuterons, tritons, and ^{3}He are predominantly emitted in the midrapidity regions [38,39] and their flow parameter values are indeed negative. At variance, for protons and alpha particles, the measured flow parameters are positive. They are emitted as much by the QP and QT as at midrapidity. But on the other hand, negative flow values are measured for fragments while the prompt emission is not the dominant process for these products. For these heavy fragments, the observed negative values cannot be explained in this way.

The second explanation attributes these negative values to the experimental methods used to extract the reaction plane. The usual method used to avoid autocorrelations, the omission of the particle of interest, leads to an anticorrelation. This induces an inversion of the reaction plane direction and then lead to the measurement of negative flow values. The amplitude of this effect increases when the flow parameter value decreases, i.e., when the incident energy is getting closer to the balance energy. This explanation is supported by the observation of negative flow values for the heaviest fragments, whereas a positive value is expected. A careful study of the autocorrelation effect shows that its manifestation results from the loss of information about the product origins for both methods.

In experimental data, these two effects are probably mixed up. They disturb the measurement of the absolute value of sideward flow, especially around the balance energy for which low flow parameter values are expected. On the other hand, the relative evolutions with incident energy, and especially the determination of the balance energy, are in agreement with previous experimental studies and theoretical calculations. It may indicate a relative robustness of the balance energy variable. In the present status, the real effect can only be studied with simulations on which the complete experimental procedure can be applied. An accurate determination of the in-medium nucleon-nucleon interaction parameters can only be achieved if the disturbances induced by the analysis methods and the experimental setup are explicitely taken into account. This requires an evolution of dynamical calculation to make possible this comparison procedure.

[1] G. F. Bertsch, W. G. Lynch, and M. B. Tsang, Phys. Lett. B **189**, 384 (1987).
[2] V. De La Mota, F. Sébille, M. Farine, B. Remaud, and P. Shuck, Phys. Rev. C **46**, 677 (1992).
[3] G. D. Westfall *et al.*, Phys. Rev. Lett. **71**, 1986 (1993).
[4] W. Q. Shen *et al.*, Nucl. Phys. **A551**, 333 (1993).
[5] R. Popescu *et al.*, Phys. Lett. B **331**, 285 (1994).
[6] J. C. Angélique *et al.*, Nucl. Phys. **A614**, 26 (1997).

[7] D. J. Magestro, W. Bauer, and G. D. Westfall, Phys. Rev. C **62**, 041603(R) (2000).
[8] J. J. Molitoris, H. Stöcker, and B. L. Winer, Phys. Rev. C **36**, 220 (1987).
[9] H. M. Xu, Phys. Rev. Lett. **67**, 2769 (1991).
[10] G. D. Westfall, Nucl. Phys. **A630**, 27c (1998).
[11] A. Ono and H. Horiuchi, Phys. Rev. C **51**, 299 (1995).
[12] B. Li, Z. Ren, C. M. Ko, and S. J. Yennello, Phys. Rev. Lett. **76**, 4492 (1996).
[13] R. Pak *et al.*, Phys. Rev. Lett. **78**, 1022 (1997).
[14] W. Reisdorf, Nucl. Phys. **A630**, 15c (1998).
[15] J. Pouthas *et al.*, INDRA Collaboration, Nucl. Instrum. Methods Phys. Res. A **357**, 418 (1995).
[16] J. Pouthas *et al.*, Nucl. Instrum. Methods Phys. Res. A **369**, 222 (1996).
[17] J. C. Steckmeyer *et al.*, in Proceedings of the XXXIII International Winter Meeting on Nuclear Physics, Bormio, Italy, edited by I. Iori, 1995, p. 255.
[18] J. Péter *et al.*, Nucl. Phys. **A519**, 611 (1990).
[19] P. Danielewicz *et al.*, Phys. Rev. C **38**, 120 (1988).
[20] J. Cugnon and D. L'Hote, Nucl. Phys. **A397**, 519 (1983).
[21] W.K. Wilson *et al.*, Phys. Rev. C **41**, 1881 (1990).
[22] C.A. Ogilvie *et al.*, Phys. Rev. C **40**, 2592 (1989).
[23] J.P. Sullivan *et al.*, Phys. Rev. B **249**, 8 (1990).
[24] C.A. Ogilvie *et al.*, Phys. Rev. C **42**, R10 (1990).
[25] D. Krofcheck *et al.*, Phys. Rev. C **46**, 1416 (1992).
[26] R. Bougault *et al.*, Nucl. Phys. **A488**, 255 (1989).
[27] L. Stuttgé *et al.*, Nucl. Phys. **A539**, 511 (1992).
[28] J.F. Lecolley *et al.*, Phys. Lett. B **354**, 202 (1995).
[29] Y. Larochelle *et al.*, Phys. Rev. C **59**, 565 (1999).
[30] J. F. Dempsey *et al.*, Phys. Rev. C **54**, 1710 (1996).
[31] J. Tõke *et al.*, Nucl. Phys. **A583**, 519 (1995).
[32] S. L. Chen *et al.*, Phys. Rev. C **54**, 2114 (1996).
[33] C. P. Montoya *et al.*, Phys. Rev. Lett. **73**, 3070 (1994).
[34] J. Lukasik *et al.*, INDRA Collaboration, Phys. Rev. C **55**, 1906 (1997).
[35] G. Casini *et al.*, Phys. Rev. Lett. **71**, 2567 (1993).
[36] A. A. Stefanini *et al.*, Z. Phys. A **351**, 167 (1995).
[37] F. Bocage *et al.*, INDRA Collaboration, Nucl. Phys. **A676**, 391 (2000).
[38] T. Lefort *et al.*, INDRA Collaboration, Nucl. Phys. **A662**, 397 (2000).
[39] D. Doré *et al.*, INDRA Collaboration, Phys. Rev. C **63**, 034612 (2001).
[40] D. Durand, Nucl. Phys. **A541**, 266 (1992).